Assessing the relationship of ancient and modern populations

Joshua G. Schraiber

Started on October 22, 2016. Compiled on November 17, 2017

Abstract

Genetic material sequenced from ancient samples is revolutionizing our understanding of the recent evolutionary past. However, ancient DNA is often degraded, resulting in low coverage, error-prone sequencing. Several solutions exist to this problem, ranging from simple approach such as selecting a read at random for each site to more complicated approaches involving genotype likelihoods. In this work, we present a novel method for assessing the relationship of an ancient sample with a modern population while accounting for sequencing error and post-mortem damage by analyzing raw read from multiple ancient individuals simultaneously. We show that when analyzing SNP data, it is better to sequence more ancient samples to low coverage: two samples sequenced to 0.5x coverage provide better resolution than a single sample sequenced to 2x coverage. We also examined the power to detect whether an ancient sample is directly ancestral to a modern population, finding that with even a few high coverage individuals, even ancient samples that are very slightly diverged from the modern population can be detected with ease. When we applied our approach to European samples, we found that no ancient samples represent direct ancestors of modern Europeans. We also found that, as shown previously, the most ancient Europeans appear to have had the smallest effective population sizes, indicating a role for agriculture in modern population growth.

1 Introduction

Ancient DNA (aDNA) is now ubiquitous in population genetics. Advances in DNA isolation (Dabney et al., 2013), library preparation (Meyer et al., 2012), bone sampling (Pinhasi et al., 2015), and sequence capture (Haak et al., 2015) make it possible to obtain genome-wide data from hundreds of samples (Haak et al., 2015; Mathieson et al., 2015; Allentoft et al., 2015; Fu et al., 2016). Analysis of these data can provide new insight into recent evolutionary processes which leave faint signatures in modern genomes, including natural selection (Schraiber et al., 2016; Jewett et al., 2016) and population replacement (Sjödin et al., 2014; Lazaridis et al., 2014).

One of the most powerful uses of ancient DNA is to assess the continuity of ancient and modern populations. In many cases, it is unclear whether populations that occupied an area in the past are the direct ancestors of the current inhabitants of that area. However, this can be next to impossible to assess using only modern genomes. Questions of population continuity and replacement have particular relevance for the spread of cultures and technology in humans (Lazaridis et al., 2016). For instance, recent work showed that modern South Americans are descended from people associated Clovis culture that inhabited North America over 10,000 years ago, further enhancing our understanding of the peopling of the Americas (Rasmussen et al., 2014).

Despite its utility in addressing difficult-to-answer questions in evolutionary biology, aDNA also has several limitations. Most strikingly, DNA decays rapidly following the death of an organism, resulting in highly fragmented, degraded starting material when sequencing (Sawyer et al., 2012). Thus, ancient data is frequently sequenced to low coverage and has a significantly higher rate of misleadingly called nucleotides than modern samples. When working with diploid data, as in aDNA extracted from plants and animals, the low coverage prevents genotypes from being called called with confidence.

Several strategies are commonly used to address the low-coverage data. One of the most common approaches is to sample a random read from each covered site and use

that as a haploid genotype call (Skoglund et al., 2012; Haak et al., 2015; Mathieson et al., 2015; Allentoft et al., 2015; Fu et al., 2016; Lazaridis et al., 2016). Many common approaches to the analyses of ancient DNA, such as the usage of F-statistics (Green et al., 2010; Patterson et al., 2012), are designed with this kind of dataset in mind. F-statistics can be interpreted as linear combinations of simpler summary statistics and can often be understood in terms of testing a tree-like structure relating populations. Nonetheless, despite the simplicity and appeal of this approach, it has several drawbacks. Primarily, it throws away reads from sites that are covered more than once, resulting in a potential loss of information from expensive, difficult-to-acquire data. Moreover, as shown by Peter (2016), F-statistics are fundamentally based on heterozygosity, which is determined by samples of size 2, and thus limited in power. Finally, these approach are also strongly impacted by sequencing error, post-mortem damage, and contamination.

On the other hand, several approaches exist to either work with genotype likelihoods or the raw read data. Genotype likelihoods are the probabilities of the read data at a site given each of the three possible diploid genotypes at that site. They can be used in calculation of population genetic statistics or likelihood functions to average over uncertainty in the genotype (Korneliussen et al., 2014). However, many such approaches assume that genotype likelihoods are fixed by the SNP calling algorithm (although they may be recalibrated to account for aDNA-specific errors, as in Jónsson et al. (2013)). However, with low coverage data, an increase in accuracy is expected if genotype likelihoods are co-estimated with other parameters of interest, due to the covariation between processes that influence read quality and genetic diversity, such as contamination.

A recent method that coestimates demographic parameters along with error and contamination rates by using genotype likelihoods showed that there can be significant power to assess the relationship of a single ancient sample to a modern population (Racimo et al., 2016). Nonetheless, they found that for very low coverage data, inferences were not reliable. Thus, they were unable to apply their method to the large

number of extremely low coverage ($<$ 1x) genomes that are available. Moreover, they were unable to explore the tradeoffs that come with a limited budget: can we learn more by sequencing fewer individuals to high coverage, or more individuals at lower coverage?

Here, we develop a novel maximum likelihood approach for analyzing low coverage ancient DNA in relation to a modern population. We work directly with raw read data and explicitly model errors due to sequencing and port-mortem damage. Crucially, our approach incorporates data from multiple individuals that belong to the same ancient population, which we show substantially increases power and reduces error in parameter estimates. We then apply our new methodology to ancient human data, and show that we can perform accurate demographic inference even from very low coverage samples by analyzing them jointly.

2 Methods

2.1 Sampling alleles in ancient populations

We assume a scenario in which allele frequencies are known with high accuracy in a modern population. Suppose that an allele is known to be at frequency $x \in (0, 1)$ in the modern population, and we wish to compute the probability of obtaining k copies of that allele in a sample of n $(0 \leq k \leq n)$ chromosomes from an ancient population. As we show in the Appendix, conditioning on the frequency of the allele in the modern population minimizes the impact of ascertainment, and allows this approach to be used for SNP capture data.

To calculate the sampling probability, we assume a simple demographic model in which the ancient individual belongs to a population that split off from the modern population τ_1 generations ago, and subsequently existed as an isolated population for τ_2 generations. Further, we assume that the modern population has effective size $N_e^{(1)}$ and that the ancient population has effective size $N_e^{(2)}$, and measure time in diffusion units,

$t_i = \tau_i/(2N_e^{(i)})$. If we know the conditional probability that an allele is at frequency y in the ancient sample, given that it is at frequency x in the modern population, denoted $f(y; x, t_1, t_2)$, then the sampling probability is simply an integral,

$$\begin{aligned} P_{n,k}(x) &= \int_0^1 \binom{n}{k} y^k (1-y)^{n-k} f(y; x, t_1, t_2) dy \\ &= \binom{n}{k} \mathbb{E}_x \left(Y^k (1-Y)^{n-k}; t_1, t_2 \right) \\ &\equiv \binom{n}{k} p_{n,k}(t_1, t_2) \end{aligned} \tag{1}$$

Thus, we must compute the binomial moments of the allele frequency distribution in the ancient population. In the Appendix, we show that this can be computed using matrix exponentiation,

$$p_{n,k}(t_1, t_2) = \left(e^{Qt_2} e^{Q^\downarrow t_1} \mathbf{h}_n \right)_i, \tag{2}$$

where $(\mathbf{v})_i$ indicates the ith element of the vector $\mathbf{v}$, $\mathbf{h}_n = ((1-x)^n, x(1-x)^{n-1}, \ldots, x^n)^T$ and Q and $Q^\downarrow$ are the sparse matrices

$$Q_{ij} = \begin{cases} \frac{1}{2} i(i-1) & \text{if } j = i-1 \\ -i(n-i) & \text{if } j = i \\ \frac{1}{2}(n-i)(n-i-1) & \text{if } j = i+1 \\ 0 & \text{else} \end{cases}$$

and

$$Q^\downarrow_{ij} = \begin{cases} \frac{1}{2} i(i-1) & \text{if } j = i-1 \\ -i(n-i+1) & \text{if } j = i \\ \frac{1}{2}(n-i+1)(n-i) & \text{if } j = i+1 \\ 0 & \text{else.} \end{cases}$$

This result has an interesting interpretation: the matrix $Q^\downarrow$ can be thought of as evolving the allele frequencies back in time from the modern population to the common

ancestor of the ancient and modern populations, while Q evolves the allele frequencies forward in time from the common ancestor to the ancient population (Fig 1).

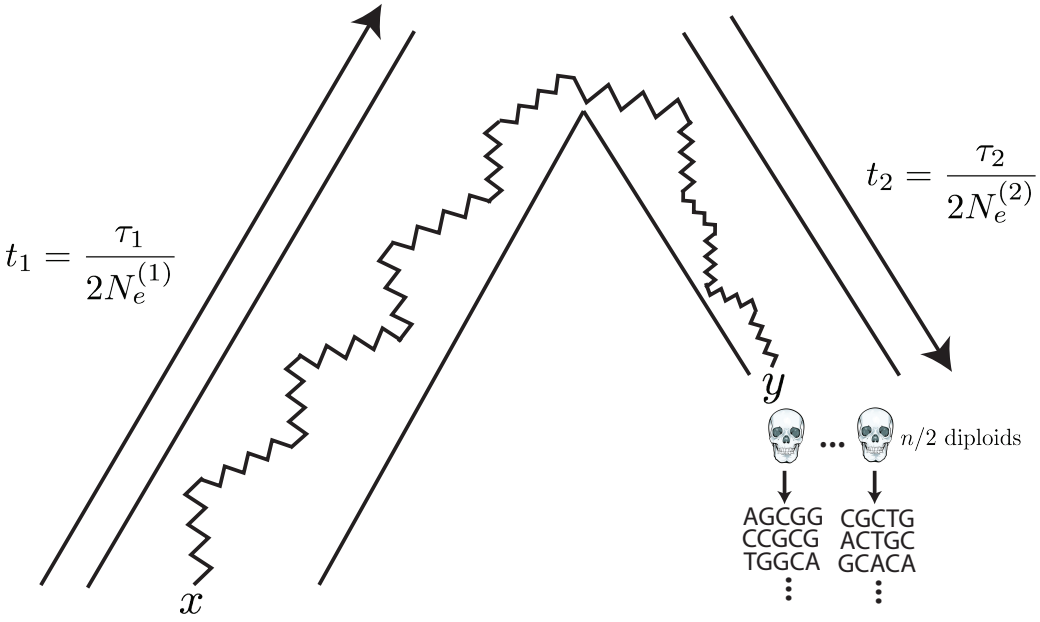

Figure 1: The generative model. Alleles are found at frequency x in the modern population and are at frequency y in the ancient population. The modern population has effective size $N_e^{(1)}$ and has evolved for τ_1 generations since the common ancestor of the modern and ancient populations, while the ancient population is of size $N_e^{(2)}$ and has evolved for τ_2 generations. Ancient diploid samples are taken and sequenced to possibly low coverage, with errors. Arrows indicate that the sampling probability can be calculated by evolving alleles *backward* in time from the modern population and then forward in time to the ancient population.

Because of the fragmentation and degradation of DNA that is inherent in obtaining sequence data from ancient individuals, it is difficult to obtain the high coverage data necessary to make high quality genotype calls from ancient individuals. To address this, we instead work directly with raw read data, and average over all the possible genotypes weighted by their probability of producing the data. Specifically, we follow Nielsen et al. (2012) in modeling the probability of the read data in the ancient population, given

the allele frequency at site l as

$$\mathbb{P}(R_l|k) = \sum_{g_{1,l}=0}^{2} \dots \sum_{g_{n,l}=0}^{2} \mathbb{I}\left(\sum_{i=1}^{m} g_{i,l} = k\right) \prod_{i=1}^{n} \binom{2}{g_{i,l}} \mathbb{P}(R_{i,l}|g_{i,l}),$$

where $R_{i,l} = (a_{i,l}, d_{i,l})$ are the counts of ancestral and derived reads in individual i at site l, $g_{i,l} \in \{0, 1, 2\}$ indicates the possible genotype of individual i at site l (i.e. $0 =$ homozygous ancestral, $1 =$ heterozygous, $2 =$ homozygous derived), and $\mathbb{P}(R_{i,l}|g_{i,l})$ is the probability of the read data at site l for individual i, assuming that the individual truly has genotype $g_{i,l}$. We use a binomial sampling with error model, in which the probability that a truly derived site appears ancestral (and vice versa) is given by ϵ. We emphasize that the parameter ϵ will capture both sequencing error as well as post-mortem damage (c.f. Racimo et al. (2016) who found that adding an additional parameter to specifically model post-mortem damage does not improve inferences). Thus,

$$\mathbb{P}(R|g) = \binom{a+d}{d} p_g^d (1-p_g)^a$$

with

$$\begin{aligned} p_0 &= \epsilon \\ p_1 &= \frac{1}{2} \\ p_2 &= 1 - \epsilon \end{aligned}$$

.

Combining these two aspects together by summing over possible allele frequencies weighted by their probabilities, we obtain our likelihood of the ancient data,

$$L(D) = \prod_{l=1}^{L} \sum_{k=0}^{n} \mathbb{P}(R_l|k) p_{n,k}(x_l). \tag{3}$$

3 Data Availability

The most recent Python implementations of the described methods are available at `www.github.com/schraiber/continuity/`. A snapshot of the code used as of the publication of the manuscript is available at `https://zenodo.org/record/1054127`.

4 Results

4.1 Impact of coverage and number of samples on inferences

To explore the tradeoff of sequencing more individuals at lower depth compared to fewer individuals at higher coverage, we performed simulations using `msprime` (Kelleher et al., 2016) combined with custom scripts to simulate error and low coverage data. Briefly, we assumed a Poisson distribution of reads at every site with mean given by the coverage, and then simulated reads by drawing from the binomial distribution described in the Methods.

First, we examined the impact of coverage and number of samples on the ability to recover the drift times in the modern and the ancient populations. Figure 2 shows results for data simulated with $t_1 = 0.02$ and $t_2 = 0.05$, corresponding to an ancient individual who died 300 generations ago from population of effective size 1000. The populations split 400 generations ago, and the modern population has an effective size of 10000. We simulated approximately 180000 SNPs by simulating 100000 500 base pair fragments. Inferences of t_1 can be relatively accurate even with only one low coverage ancient sample (Figure 2A). However, inferences of t_2 benefit much more from increasing the number of ancient samples, as opposed to coverage (Figure 2B). Supplementary Table 1 shows that there is very little change in the average estimated parameter, indicating that most of the change in RMSE is due to decreased sampling variance. Thus, two individuals sequenced to 0.5x coverage have a much lower error than a single individual sequenced to 2x coverage, even though there is very little bias in either case. To explore this effect further, we derived the sampling probability of alleles

covered by exactly one sequencing read (see Appendix). We found that sites covered only once have no information about t_2, suggesting that evidence of heterozygosity is very important for inferences about t_2. Finally, though we showed through simulation that there is sufficient power to disentangle t_1 from t_2, estimates of these parameters are negatively correlated, due to the necessity of fitting the total drift time $t_1 + t_2$ (Supplementary Figure 1).

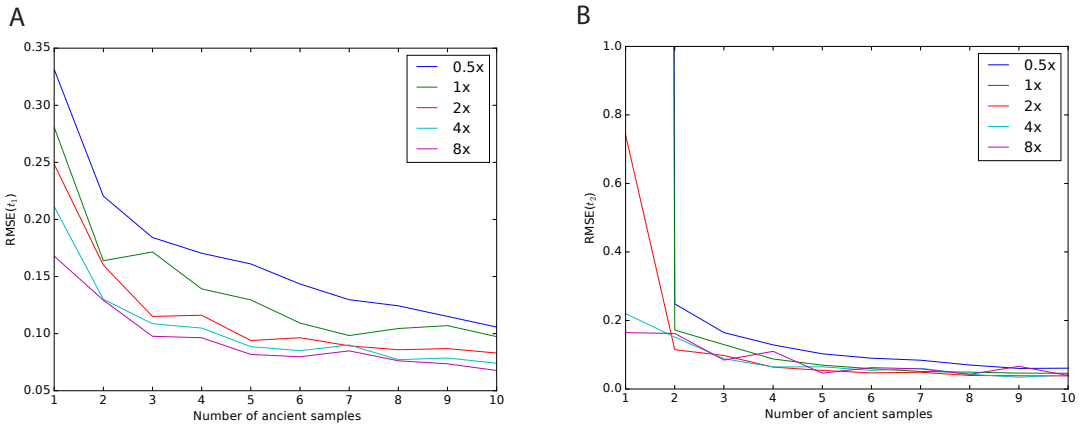

Figure 2: Impact of sampling scheme on parameter estimation error. In each panel, the x axis represents the number of simulated ancient samples, while the y axis shows the relative root mean square error for each parameter. Each different line corresponds to individuals sequenced to different depth of coverage. Panel A shows results for t_1 while panel B shows results for t_2. Simulated parameters are $t_1 = 0.02$ and $t_2 = 0.05$.

We next examined the impact of coverage and sampling on the power to reject the hypothesis that the ancient individuals came from a population that is directly ancestral to the modern population. We analyzed both low coverage (0.5x) and higher coverage (4x) datasets consisting of 1 (for both low and high coverage samples) or 5 individuals (only for low coverage). We simulated data with parameters identical to the previous experiment, except we now examined the impact of varying the age of the ancient sample from 0 generations ago through to the split time with the modern population. We then performed a likelihood ratio test comparing the null model of continuity, in which $t_2 = 0$, to a model in which the ancient population is not continuous.

Figure 3 shows the power of the likelihood ratio test. For a single individual sequenced to low coverage, we see that the test only has power for very recently sampled ancient individuals (i.e. samples that are highly diverged from the modern population). However, the power increases dramatically as the number of individuals or the coverage per individual is increased; sequencing 5 individuals to 0.5x coverage results in essentially perfect power to reject continuity. Nonetheless, for samples that are very close to the divergence time, it will be difficult to determine if they are ancestral to the modern population or not, because differentiation is incomplete.

4.2 Impact of admixture

We examined two possible ways that admixture can result in violations of the model to assess their impact on inference. In many situations, there may have been secondary contact between the population from which the ancient sample is derived and the modern population used as a reference. We performed simulations of this situation by modifying the simulation corresponding to Figure 2 (300 generation old ancient sample from population of size 1000 split from a population of size 10000 400 generations ago) to include subsequent admixture from the ancient population to the modern population 200 generations ago (NB: this admixture occurred *more recently* than the ancient sample). In Figure 4, we show the results for admixture proportions ranging from 0 to 50%. Counterintuitively, estimates of t_1 initially *decrease* before again increasing. This is likely a result of the increased heterozygosity caused by admixture, which acts to artificially inflate the effective size of the modern population, and thus decrease t_1. As expected, t_2 is estimated to be smaller the more admixture there is; indeed, for an admixture rate of 100%, the modern and ancient samples are continuous. The impact on t_2 appears to be linear, and is well approximated by $(1 - f)t_2$ if the admixture fraction is f.

In other situations, there may be admixture from an unsampled "ghost" population into the modern population. If the ghost admixture is of a high enough proportion, it

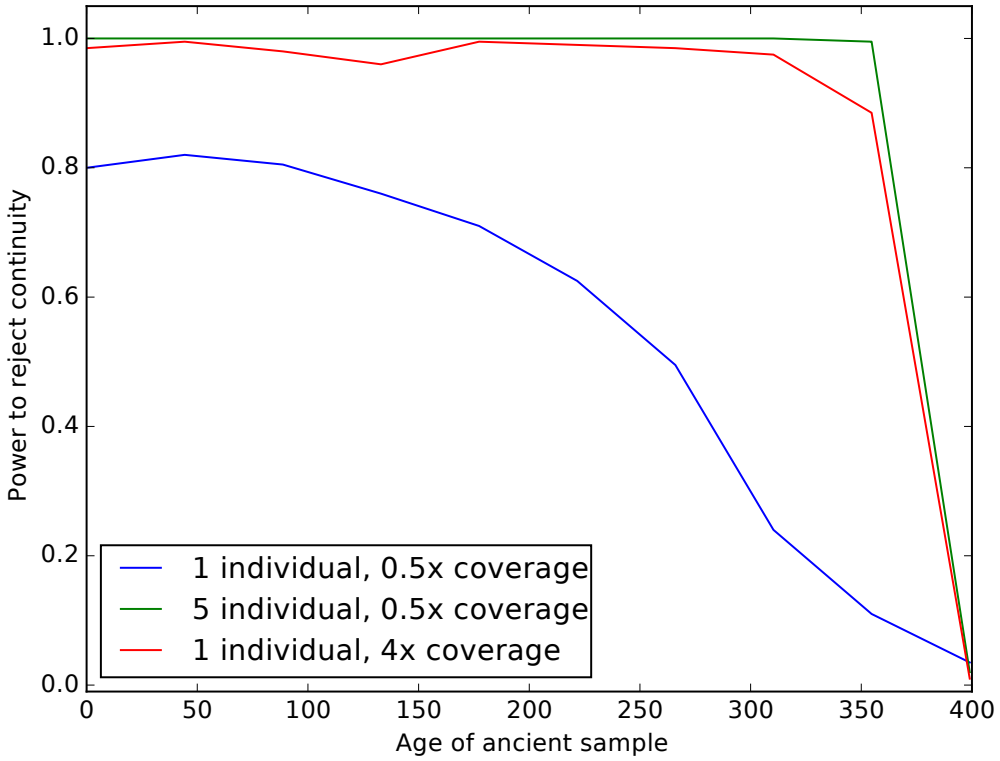

Figure 3: Impact of sampling scheme on rejecting population continuity. The x axis represents the age of the ancient sample in generations, with 0 indicating a modern sample and 400 indicating a sample from exactly at the split time 400 generations ago. The y axis shows the proportion of simulations in which we rejected the null hypothesis of population continuity. Each line shows different sampling schemes, as explained in the legend.

is likely to cause a sample that is in fact a member of a directly ancestral population to not appear to be ancestral. We explored this situation by augmenting our simulations in which the ancient sample is continuous with an outgroup population diverged from the modern population 0.04 time units ago (corresponding to 800 generations ago) and contributed genes to the modern population 0.01 time units ago (corresponding to 200 generations ago). We then assessed the impact on rejecting continuity using the likelihood ratio test (Figure 5). As expected, we see that low-power sampling strategies

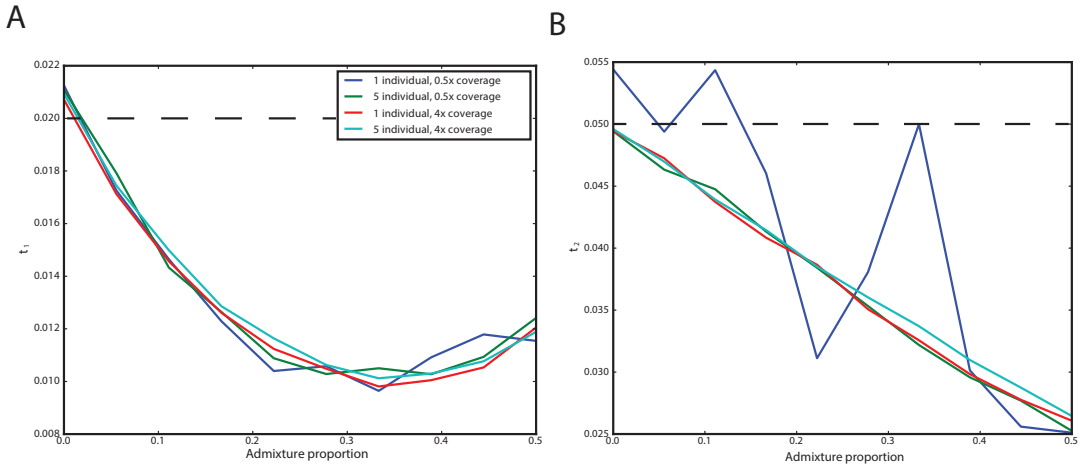

Figure 4: Impact of admixture from the ancient population on inferred parameters. The x axis shows the admixture proportion and the y axis shows the average parameter estimate across simulations. Each line corresponds to a different sampling strategy, as indicated in the legend. Panel A shows results for t_1 and Panel B shows results for t_2. The true values of $t_1 = 0.02$ and $t_2 = 0.05$ are indicated by dashed lines.

(such as a single individual sequenced to low coverage) are very minimally impacted by ghost admixture. However, for more powerful sampling strategies, moderate rates of ghost admixture ($\sim 10\%$) result in rejection of continuity.

4.3 Impact of contamination

We also explored the impact of foreign DNA contamination on inferences made using this approach. Briefly, we modified the simulations to include a chance c of a read being from a modern sample instead of the ancient sample when simulating reads. We again simulated data corresponding to Figure 2, with a 300 generation old ancient sample from population of size 1000 split from a population of size 10000 400 generations ago. In Figure 6, we see that relatively modest amounts of contamination can result in estimating zero or near-zero drift times. Interestingly, for the same contamination fraction, higher coverage samples are impacted slightly less. Together, this suggests that contamination will result in samples to be falsely inferred to be directly continuous

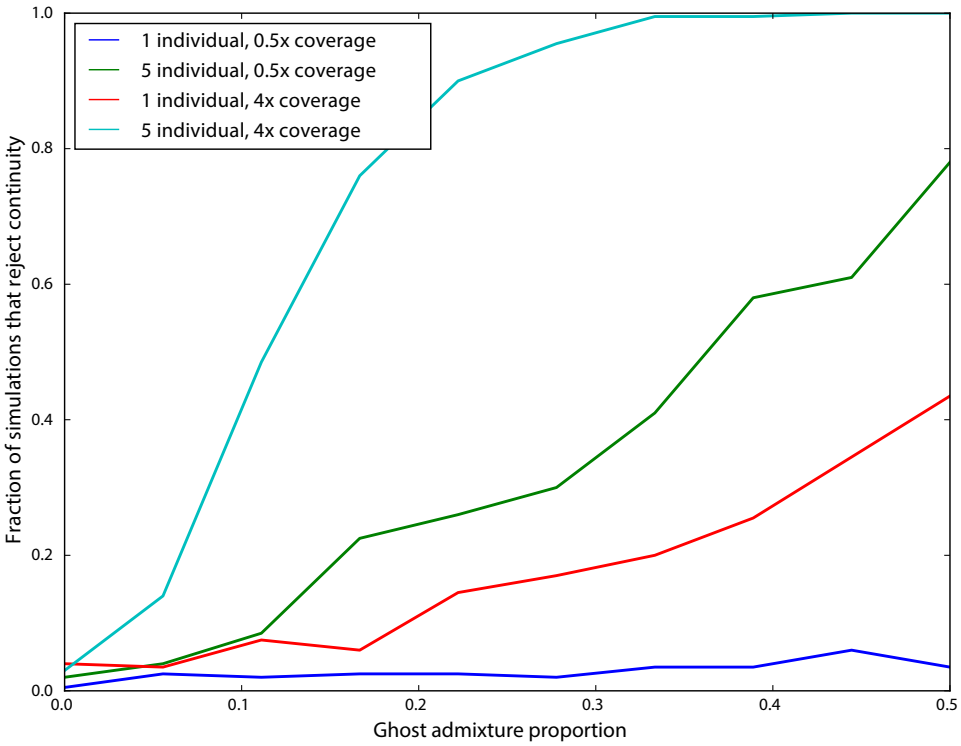

Figure 5: Impact of ghost admixture on rejecting continuity. The x axis shows the admixture proportion from the ghost population, and the y axis shows the fraction of simulations in which continuity was rejected. Each line corresponds to a different sampling strategy, as indicated in the legend.

with the modern population.

4.4 Application to ancient humans

We applied our approach to ancient human data from Mathieson et al. (2015), which is primarily derived from a SNP capture approach that targeted 1.2 million SNPs. Based on sampling location and associated archeological materials, the individuals were grouped into *a priori* panels, which we used to specify population membership when analyzing individuals together. We analyzed all samples for their relationship to

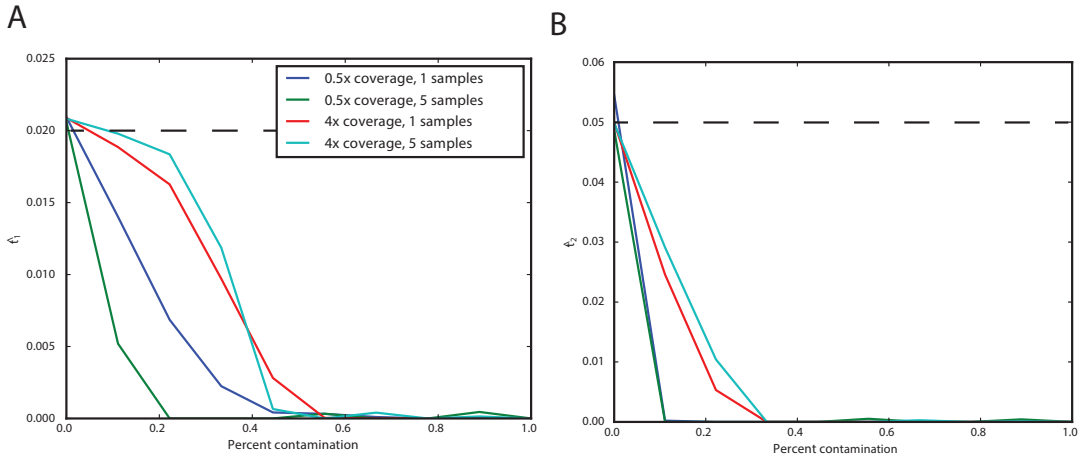

Figure 6: Impact of contamination on parameter inference. The x axis shows the contamination fraction, and the y axis shows the average parameter estimate from simulations. Each line corresponds to a different sampling strategy, as indicated in the legend. Panel A shows t_1, and Panel B shows t_2. Dashed lines indicate the true values of $t_1 = 0.02$ and $t_2 = 0.05$

the CEU individuals from the 1000 Genomes Project (Consortium, 2015). Based on our results that suggested that extremely low coverage samples would yield unreliable estimates, we excluded panels that are composed of only a single individual sequenced to less than 2x coverage.

We computed maximum likelihood estimates of t_1 and t_2 for individuals as grouped into populations (Figure 7A; Table 1). We observe that t_2 is significantly greater than 0 for all populations according to the likelihood ratio test. Thus, none of these populations are consistent with directly making up a large proportion of the ancestry of modern CEU individuals. Strikingly, we see that $t_2 \gg t_1$, despite the fact these samples died in the past, and thus they belonged to a lineage that must have existed for fewer generations since the population split than the modern samples. This suggests that all of the ancient populations are characterized by extremely small effective population sizes.

We further explored the relationship between the dates of the ancient samples and

pop	cov	date	t_1	t_2	lnL	t_1 (cont)	lnL (cont)
Alberstedt_LN	12.606	4417.000	0.005	0.013	-779411.494	0.006	-779440.143
Anatolia_Neolithic	3.551	8317.500	0.010	0.042	-9096440.714	0.044	-9106156.877
Baalberge_MN	0.244	5684.333	0.001	0.071	-201575.306	0.007	-201750.419
Bell_Beaker_Germany	1.161	4308.444	0.003	0.010	-1834486.744	0.008	-1834652.858
BenzigerodeHeimburg_LN	0.798	4209.750	0.003	0.032	-346061.545	0.007	-346134.356
Corded_Ware_Germany	2.250	4372.833	0.005	0.023	-2139002.723	0.017	-2139858.192
Esperstedt_MN	30.410	5238.000	0.005	0.029	-975890.329	0.009	-976047.889
Halberstadt_LBA	5.322	3082.000	0.003	0.015	-558966.522	0.004	-558993.078
Hungary_BA	3.401	3695.750	0.004	0.023	-789754.969	0.010	-789939.889
Hungary_CA	5.169	4869.500	0.005	0.037	-504413.094	0.010	-504549.603
Hungary_EN	4.033	7177.000	0.007	0.036	-3478429.262	0.033	-3481855.461
Hungary_HG	5.807	7763.000	0.000	0.147	-469887.471	0.015	-471652.083
Iberia_Chalcolithic	1.686	4630.625	0.005	0.037	-2351769.869	0.028	-2354249.543
Iberia_EN	4.875	7239.500	0.005	0.053	-1483274.628	0.030	-1485675.934
Iberia_MN	5.458	5765.000	0.004	0.039	-1491407.962	0.023	-1492793.179
Iberia_Mesolithic	21.838	7830.000	0.009	0.141	-720759.133	0.030	-723091.935
Karelia_HG	2.953	7265.000	0.008	0.125	-652952.676	0.033	-655352.439
LBK_EN	2.894	7123.429	0.007	0.039	-3656617.954	0.033	-3660838.639
Motala_HG	2.207	7729.500	0.003	0.126	-1477338.076	0.068	-1489573.895
Poltavka	2.211	4684.500	0.008	0.029	-1334662.071	0.020	-1335358.630
Potapovka	0.267	4076.500	0.004	0.063	-220112.816	0.011	-220251.379
Samara_Eneolithic	0.463	6615.000	0.007	0.078	-362161.674	0.020	-362689.209
Scythian_IA	3.217	2305.000	0.012	0.011	-492961.306	0.013	-492973.694
Srubnaya	1.662	3653.273	0.004	0.015	-2578065.957	0.013	-2578645.731
Srubnaya_Outlier	0.542	3704.500	0.006	0.019	-285828.766	0.008	-285851.523
Unetice_EBA	1.320	4024.786	0.002	0.012	-1676798.610	0.008	-1677026.310
Yamnaya_Samara	1.937	4990.500	0.008	0.033	-2440183.354	0.028	-2442192.801

Table 1: Details of populations included in analysis. "pop" is population name, "cov" is mean coverage of individuals in the population, "date" is mean date of individuals in the population, "t_1" is the maximum likelihood estimate of t_1 in the full model, "t_2" is the maximum likelihood estimate of t_2 in the full model, "LnL" is the maximum likelihood value in the full model, "t_1 (cont)" is the maximum likelihood estimate of t_1 in the model where $t_2 = 0$, "LnL" is the maximum likelihood value in the model where $t_2 = 0$.

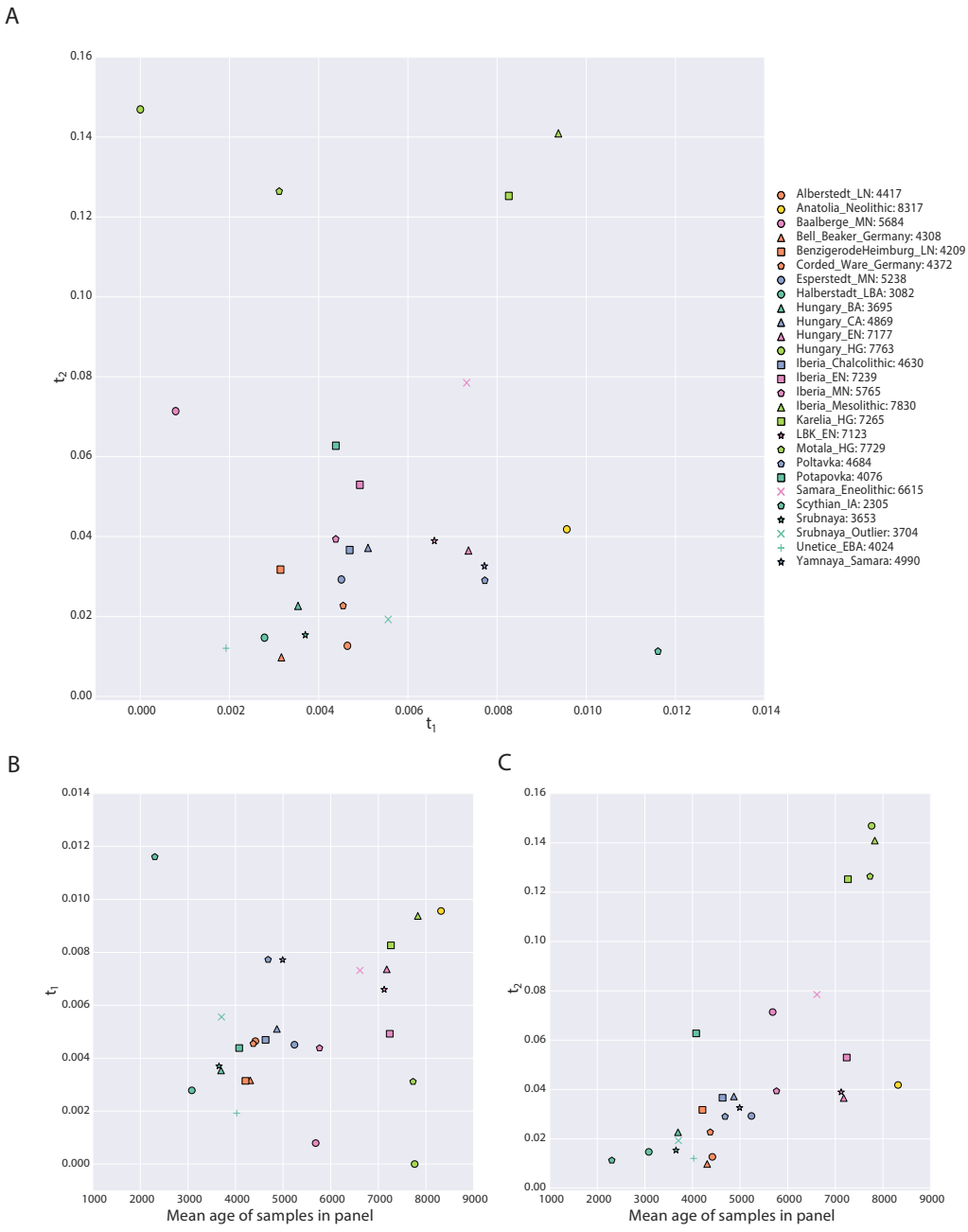

Figure 7: Parameters of the model inferred from ancient West Eurasian samples. Panel A shows t_1 on the x-axis and t_2 on the y-axis, with each point corresponding to a population as indicated in the legend. Numbers in the legend correspond to the mean date of all samples in the population. Panels B and C show scatterplots of the mean age of the samples in the population (x-axis) against t_1 and t_2, respectively. Points are described by the same legend as Panel A.

the parameters of the model by plotting t_1 and t_2 against the mean sample date of all samples in that population (Figure 7B, C). We expected to find that t_1 correlated with sample age, under the assumption that samples were members of relatively short-lived populations that diverged from the "main-stem" of CEU ancestry. Instead, we see no correlation between t_1 and sample time, suggesting that the relationship of these populations to the CEU is complicated and not summarized well by the age of the samples. On the other hand, we see a strong positive correlation between t_2 and sampling time ($p < 1 \times 10^{-4}$). Because t_2 is a compound parameter, it is difficult to directly interpret this relationship. However, it is consistent with the most ancient samples belonging to populations with the smallest effective sizes, consistent with previous observations (Skoglund et al., 2014).

Finally, we examined the impact of grouping individuals into populations in real data. We see that estimates of t_1 for low coverage samples are typically lower when analyzed individually than when pooled with other individuals of the same panel (Figure 8A); because Supplementary Table 1 shows that there is no downward bias in t_1 for low coverage, this suggests that there may be some heterogeneity in these panels. On the other hand, there is substantial bias toward overestimating t_2 when analyzing samples individually, particularly for very low coverage samples (Figure 8B). This again shows that for estimates that rely on heterozygosity in ancient populations, pooling many low coverage individuals can significantly improve estimates.

5 Discussion

Ancient DNA (aDNA) presents unique opportunities to enhance our understanding of demography and selection in recent history. However, it also comes equipped with several challenges, due to postmortem DNA damage (Sawyer et al., 2012). Several strategies have been developed to deal with the low quality of aDNA data, from relatively simple options like sampling a read at random at every site (Green et al., 2010) to more complicated methods making use of genotype likelihoods (Racimo et al., 2016).

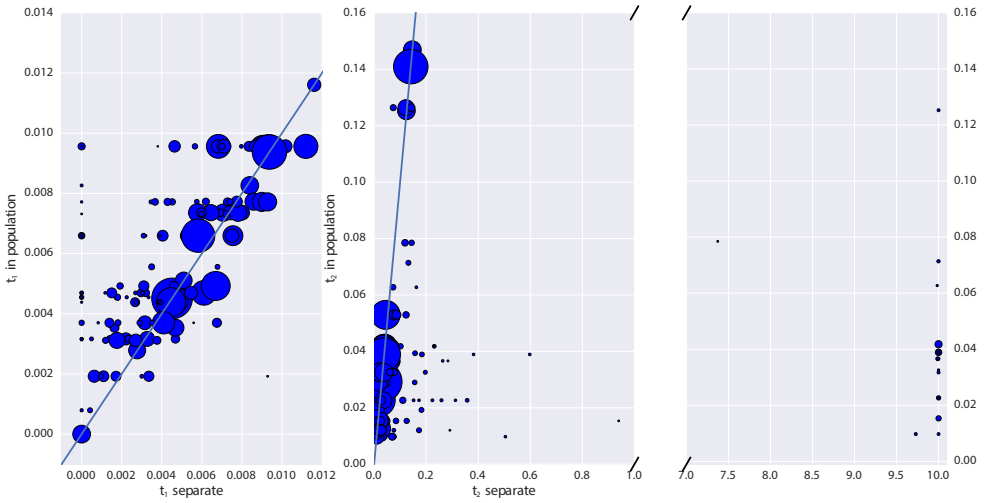

Figure 8: Impact of pooling individuals into populations when estimating model parameters from real data. In both panels, the x-axis indicates the parameter estimate when individuals are analyzed separately, while the y-axis indicates the parameter estimate when individuals are grouped into populations. Size of points is proportional to the coverage of each individual. Panel A reports the impact on estimation of t_1, while Panel B reports the impact on t_2. Note that Panel B has a broken x-axis. Solid lines in each figure indicate $y = x$.

Here, we presented a novel maximum likelihood approach for making inferences about how ancient populations are related to modern populations by analyzing read counts from multiple ancient individuals and explicitly modeling relationship between the two populations. We explicitly condition on the allele frequency in a modern population; as we showed in the appendix, this renders our method robust to ascertainment in modern samples. Thus, it can be used with SNP capture data. Moreover, confidence intervals can be calculated using a nonparametric bootstrap, although this will be computational intensive for large ancient panels, such as those considered in this manuscript. Using this approach, we examined some aspects of sampling strategy for aDNA analysis and we applied our approach to ancient humans.

We found that sequencing many individuals from an ancient population to low

coverage (.5-1x) can be a significantly more cost effective strategy than sequencing fewer individuals to relatively high coverage. For instance, we saw from simulations that far more accurate estimates of the drift time in an ancient population can be obtained by pooling 2 individuals at 0.5x coverage than by sequencing a single individual to 2x coverage (Figure 2). We saw this replicated in our analysis of the real data: low coverage individuals showed a significant amount of variation and bias in estimating the model parameters that was substantially reduced when individuals were analyzed jointly in a population (Figure 8). To explore this further, we showed that sites sequenced to 1x coverage in a single individual retain no information about the drift time in the ancient population. This can be intuitively understood because the drift time in the ancient population is strongly related the amount of heterozygosity in the ancient population: an ancient population with a longer drift time will have lower heterozygosity at sites shared with a modern population. When a site is only sequenced once in a single individual, there is no information about the heterozygosity of that site. We also observed a pronounced upward bias in estimates of the drift time in the ancient population from low coverage samples. We speculate that this is due to the presence of few sites covered more than once being likely to be homozygous, thus deflating the estimate of heterozygosity in the ancient population. Thus, for analysis of SNP data, we recommend that aDNA sampling be conduced to maximize the number of individuals from each ancient population that can be sequenced to $\sim$1x, rather than attempting to sequence fewer individuals to high coverage. This suggestion can be complicated when samples have vastly different levels of endogenous DNA, where it may be cost effective to sequence high quality samples to higher coverage. In that case, we recommend sequencing samples to at least 3-4x coverage; as evidenced by Figures 2 and 3, single samples at $<$4x coverage provide extremely limited information about the drift time in the ancient population and thus little power to reject continuity.

When we looked at the impact of model misspecification, we saw several important patterns. First, the influence of admixture from the ancient population on inferences of t_2 is approximately linear, suggesting that if there are estimates of the amount of

admixture between the modern and ancient population, a bias-corrected estimate of t_2 could be produced (Figure 4B). The impact on inference of t_1 is more complicated: admixture actually *reduces* estimates of t_1 (Figure 4A). This is likely because admixture increases the heterozygosity in the modern population, thus causing the amount of drift time to seem reduced. In both cases, the bias is not impacted by details of sampling strategy, although the variance of estimates is highly in a way consistent with Figure 2.

Of particular interest in many studies of ancient populations is the question of direct ancestry: are the ancient samples members of a population that contributed substantially to a modern population? We emphasize that this does not mean that the particular samples were direct ancestors of any modern individuals; indeed, this is exceedingly unlikely for old samples (Rohde et al., 2004; Chang, 1999; Baird et al., 2003; Donnelly, 1983). Instead, we are asking whether an ancient sample was a member of a population that is directly continuous with a modern population. Several methods have been proposed to test this question, but thus far they have been limited to many individuals sequenced at a single locus (Sjödin et al., 2014) or to a single individual with genome-wide data (Rasmussen et al., 2014). Our approach provides a rigorous, maximum likelihood framework for testing questions of population continuity using multiple low coverage ancient samples. We saw from simulations (Figure 3) that data from single, low coverage individuals result in very little power to reject the null hypothesis of continuity unless the ancient sample is very recent (i.e. it has been diverged from the modern population for a long time). Nonetheless, when low coverage individuals are pooled together, or a single high coverage individual is used, there is substantial power to reject continuity for all but the most ancient samples (i.e. samples dating from very near the population split time).

Because many modern populations may have experienced admixture from unsampled "ghost" populations, we also performed simulations to test the impact of ghost admixture on the probability of falsely rejecting continuity. We find that single ancient samples do not provide sufficient power to reject continuity even for high levels of

ghost admixture, while increasingly powerful sampling schemes, adding more individuals or higher coverage per individual, reject continuity at higher rates. However, in these situations, whether we regard rejection of continuity as a false or true discovery is somewhat subjective: how much admixture from an outside population is required before considering a population to not be directly ancestral? In future work it will be extremely important to estimate the "maximum contribution" of the population an ancient sample comes from (c.f Sjödin et al. (2014)).

To gain new insights from empirical data, we applied our approach to ancient samples throughout Europe. Notably, we rejected continuity for all populations that we analyzed. This is unsurprising, given that European history is extremely complicated and has been shaped by many periods of admixture (Lazaridis et al., 2014; Haak et al., 2015; Lazaridis et al., 2016). Thus, modern Europeans have experienced many periods of "ghost" admixture (relative to any particular ancient sample). Nonetheless, our results show that none of these populations are even particularly close to directly ancestral, as our simulations have shown that rejection of continuity will not occur with low levels of ghost admixture.

Secondly, we observed that the drift time in the ancient population was much larger than the drift time in the modern population. Assuming that the ancient sample were a contemporary sample, the ratio t_1/t_2 is an estimator of the ratio $N_e^{(2)}/N_e^{(1)}$; in fact, because the ancient sample existed for fewer generations since the common ancestor of the ancient and modern populations, t_1/t_2 acts as an upper bound on $N_e^{(2)}/N_e^{(1)}$. Moreover, this is unlikely to be due to unmodeled error in the ancient samples: error would be expected increase the heterozygosity in the ancient sample, and thus *decrease* our estimates of t_2. Another potential complication is the fact that modern Europeans are a mixture of multiple ancestral populations (Lazaridis et al., 2014; Haak et al., 2015). As shown through simulation, admixture increases heterozygosity in the modern population and thus decreases estimates of t_1. However, even very large amounts of ghost admixture did not result in the order-of-magnitude differences we see in the real data, suggesting that ghost admixture cannot account for all the discrepancy

between modern and ancient N_e. Thus, we find strong support for the observation that ancient Europeans were often members of small, isolated populations (Skoglund et al., 2014). We interpret these these two results together as suggestive that many ancient samples found thus far in Europe were members of small populations that ultimately went locally extinct. Nonetheless, there may be many samples that belonged to larger metapopulations, and further work is necessary to specifically examine those cases.

We further examined the effective sizes of ancient populations through time by looking for a correlation between the age of the ancient populations and the drift time leading to them (Figure 7C). We saw a strong positive correlation, and although this drift time is a compound parameter, which complicates interpretations, it appears that the oldest Europeans were members of the smallest populations, and that effective population size has grown through time as agriculture spread through Europe.

We anticipate the further development of methods that explicitly account for differential drift times in ancient and modern samples will become important as aDNA research becomes even more integrating into population genomics. This is because many common summary methods, such as the use of Structure (Pritchard et al., 2000) and Admixture (Alexander et al., 2009), are sensitive to differential amounts of drift between populations (Falush et al., 2016). As we've shown in ancient Europeans, ancient samples tend to come from isolated subpopulations with a large amount of drift, thus confounding such summary approaches. Moreover, standard population genetics theory shows that allele frequencies are expected to be deterministically lower in ancient samples, even if they are direct ancestors of a modern population. Intuitively, this arises because the alleles must have arisen at some point from new mutations, and thus were at lower frequencies in the past. A potentially fruitful avenue to combine these approaches moving forward may be to separate regions of the genome based on ancestry components, and assess the ancestry of ancient samples relative to specific ancestry components, rather than to genomes as a whole.

Our current approach leaves several avenues for improvement. We use a relatively simple error model that wraps up both post-mortem damage and sequencing error

into a single parameter. While Racimo et al. (2016) shows that adding an additional parameter for PMD-related error does not significantly change results, the recent work of Kousathanas et al. (2017) shows that building robust error models is challenging and essential to estimating heterozygosity properly. Although our method is robust to non-constant demography because we consider only alleles that are segregating in both the modern and the ancient population, we are losing information by not modeling new mutations that arise in the ancient population. Similarly, we only consider a single ancient population at a time, albeit with multiple samples. Ideally, ancient samples would be embedded in complex demographic models that include admixture, detailing their relationships to each other and to modern populations (Patterson et al., 2012; Lipson and Reich, 2017). However, inference of such complex models is difficult, and though there has been some progress in simplified cases (Lipson et al., 2014; Pickrell and Pritchard, 2012), it remains an open problem due to the difficult of simultaneously inferring a non-tree-like topology along with demographic parameters. Software such as `momi` (Kamm et al., 2016) that can compute the likelihood of SNP data in an admixture graph may be able to be used to integrate over genotype uncertainty in larger settings than considered here.

6 Acknowledgments

We wish to thank Melinda Yang, Iain Mathieson, Pontus Skoglund, and Fernando Racimo for several discussions during the conception of this work that greatly improved its scope and rigor. We are grateful to Fernando Racimo and Benjamin Vernot for comments on early versions of this work that significantly improved its quality. We also appreciate comments on the preprint from Alex Kim and Aylwyn Scally. We would also like to thank Tamara Broderick for several stimulating discussions about clustering that ultimately didn't result in any interesting application to ancient DNA.

References

David H Alexander, John Novembre, and Kenneth Lange. Fast model-based estimation of ancestry in unrelated individuals. *Genome research*, 19(9):1655–1664, 2009.

Morten E Allentoft, Martin Sikora, Karl-Göran Sjögren, Simon Rasmussen, Morten Rasmussen, Jesper Stenderup, Peter B Damgaard, Hannes Schroeder, Torbjörn Ahlström, Lasse Vinner, et al. Population genomics of bronze age eurasia. *Nature*, 522(7555):167–172, 2015.

SJE Baird, NH Barton, and AM Etheridge. The distribution of surviving blocks of an ancestral genome. *Theoretical population biology*, 64(4):451–471, 2003.

Joseph T Chang. Recent common ancestors of all present-day individuals. *Advances in Applied Probability*, 31(4):1002–1026, 1999.

1000 Genomes Project Consortium. A global reference for human genetic variation. *Nature*, 526(7571):68–74, 2015.

Jesse Dabney, Matthias Meyer, and Svante Pääbo. Ancient dna damage. *Cold Spring Harbor perspectives in biology*, 5(7):a012567, 2013.

Kevin P Donnelly. The probability that related individuals share some section of genome identical by descent. *Theoretical population biology*, 23(1):34–63, 1983.

Warren J Ewens. *Mathematical population genetics 1: theoretical introduction*, volume 27. Springer Science & Business Media, 2012.

Daniel Falush, Lucy van Dorp, and Daniel Lawson. A tutorial on how (not) to over-interpret structure/admixture bar plots. *bioRxiv*, page 066431, 2016.

Qiaomei Fu, Cosimo Posth, Mateja Hajdinjak, Martin Petr, Swapan Mallick, Daniel Fernandes, Anja Furtwängler, Wolfgang Haak, Matthias Meyer, Alissa Mittnik, et al. The genetic history of ice age europe. *Nature*, 2016.

Richard E Green, Johannes Krause, Adrian W Briggs, Tomislav Maricic, Udo Stenzel, Martin Kircher, Nick Patterson, Heng Li, Weiwei Zhai, Markus Hsi-Yang Fritz, et al. A draft sequence of the neandertal genome. *science*, 328(5979):710–722, 2010.

RC Griffiths. The frequency spectrum of a mutation, and its age, in a general diffusion model. *Theoretical population biology*, 64(2):241–251, 2003.

Wolfgang Haak, Iosif Lazaridis, Nick Patterson, Nadin Rohland, Swapan Mallick, Bastien Llamas, Guido Brandt, Susanne Nordenfelt, Eadaoin Harney, Kristin Stewardson, et al. Massive migration from the steppe was a source for indo-european languages in europe. *Nature*, 522(7555):207–211, 2015.

Ethan M Jewett, Matthias Steinrücken, and Yun S Song. The effects of population size histories on estimates of selection coefficients from time-series genetic data. *Molecular Biology and Evolution*, page msw173, 2016.

Hákon Jónsson, Aurélien Ginolhac, Mikkel Schubert, Philip LF Johnson, and Ludovic Orlando. mapdamage2. 0: fast approximate bayesian estimates of ancient dna damage parameters. *Bioinformatics*, 29(13):1682–1684, 2013.

John A Kamm, Jonathan Terhorst, and Yun S Song. Efficient computation of the joint sample frequency spectra for multiple populations. *Journal of Computational and Graphical Statistics*, (just-accepted):1–37, 2016.

Samuel Karlin and Howard E Taylor. *A second course in stochastic processes*. Elsevier, 1981.

Jerome Kelleher, Alison M Etheridge, and Gilean McVean. Efficient coalescent simulation and genealogical analysis for large sample sizes. *PLoS Comput Biol*, 12(5): e1004842, 2016.

Thorfinn Sand Korneliussen, Anders Albrechtsen, and Rasmus Nielsen. Angsd: analysis of next generation sequencing data. *BMC bioinformatics*, 15(1):356, 2014.

Athanasios Kousathanas, Christoph Leuenberger, Vivian Link, Christian Sell, Joachim Burger, and Daniel Wegmann. Inferring heterozygosity from ancient and low coverage genomes. *Genetics*, 205(1):317–332, 2017.

Iosif Lazaridis, Nick Patterson, Alissa Mittnik, Gabriel Renaud, Swapan Mallick, Karola Kirsanow, Peter H Sudmant, Joshua G Schraiber, Sergi Castellano, Mark Lipson, et al. Ancient human genomes suggest three ancestral populations for present-day europeans. *Nature*, 513(7518):409–413, 2014.

Iosif Lazaridis, Dani Nadel, Gary Rollefson, Deborah C Merrett, Nadin Rohland, Swapan Mallick, Daniel Fernandes, Mario Novak, Beatriz Gamarra, Kendra Sirak, et al. Genomic insights into the origin of farming in the ancient near east. *Nature*, 536 (7617):419–424, 2016.

Mark Lipson and David Reich. Working model of the deep relationships of diverse modern human genetic lineages outside of africa. *Molecular Biology and Evolution*, page msw293, 2017.

Mark Lipson, Po-Ru Loh, Nick Patterson, Priya Moorjani, Ying-Chin Ko, Mark Stoneking, Bonnie Berger, and David Reich. Reconstructing austronesian population history in island southeast asia. *Nature communications*, 5, 2014.

Iain Mathieson, Iosif Lazaridis, Nadin Rohland, Swapan Mallick, Nick Patterson, Songül Alpaslan Roodenberg, Eadaoin Harney, Kristin Stewardson, Daniel Fernandes, Mario Novak, et al. Genome-wide patterns of selection in 230 ancient eurasians. *Nature*, 528(7583):499–503, 2015.

Matthias Meyer, Martin Kircher, Marie-Theres Gansauge, Heng Li, Fernando Racimo, Swapan Mallick, Joshua G Schraiber, Flora Jay, Kay Prüfer, Cesare De Filippo, et al. A high-coverage genome sequence from an archaic denisovan individual. *Science*, 338 (6104):222–226, 2012.

493 Rasmus Nielsen and James Signorovitch. Correcting for ascertainment biases when
494 analyzing snp data: applications to the estimation of linkage disequilibrium. *Theo-*
495 *retical population biology*, 63(3):245–255, 2003.

496 Rasmus Nielsen, Thorfinn Korneliussen, Anders Albrechtsen, Yingrui Li, and Jun
497 Wang. Snp calling, genotype calling, and sample allele frequency estimation from
498 new-generation sequencing data. *PloS one*, 7(7):e37558, 2012.

499 Nick Patterson, Priya Moorjani, Yontao Luo, Swapan Mallick, Nadin Rohland, Yiping
500 Zhan, Teri Genschoreck, Teresa Webster, and David Reich. Ancient admixture in
501 human history. *Genetics*, 192(3):1065–1093, 2012.

502 Benjamin M Peter. Admixture, population structure, and f-statistics. *Genetics*, 202
503 (4):1485–1501, 2016.

504 Joseph K Pickrell and Jonathan K Pritchard. Inference of population splits and mix-
505 tures from genome-wide allele frequency data. *PLoS Genet*, 8(11):e1002967, 2012.

506 Ron Pinhasi, Daniel Fernandes, Kendra Sirak, Mario Novak, Sarah Connell, Songül
507 Alpaslan-Roodenberg, Fokke Gerritsen, Vyacheslav Moiseyev, Andrey Gromov, Pál
508 Raczky, et al. Optimal ancient dna yields from the inner ear part of the human
509 petrous bone. *PloS one*, 10(6):e0129102, 2015.

510 Jonathan K Pritchard, Matthew Stephens, and Peter Donnelly. Inference of population
511 structure using multilocus genotype data. *Genetics*, 155(2):945–959, 2000.

512 Fernando Racimo, Gabriel Renaud, and Montgomery Slatkin. Joint estimation of
513 contamination, error and demography for nuclear dna from ancient humans. *PLoS*
514 *Genet*, 12(4):e1005972, 2016.

515 Morten Rasmussen, Sarah L Anzick, Michael R Waters, Pontus Skoglund, Michael De-
516 Giorgio, Thomas W Stafford Jr, Simon Rasmussen, Ida Moltke, Anders Albrechtsen,
517 Shane M Doyle, et al. The genome of a late pleistocene human from a clovis burial
518 site in western montana. *Nature*, 506(7487):225–229, 2014.

Douglas LT Rohde, Steve Olson, and Joseph T Chang. Modelling the recent common ancestry of all living humans. *Nature*, 431(7008):562, 2004.

Susanna Sawyer, Johannes Krause, Katerina Guschanski, Vincent Savolainen, and Svante Pääbo. Temporal patterns of nucleotide misincorporations and dna fragmentation in ancient dna. *PloS one*, 7(3):e34131, 2012.

Joshua G Schraiber, Steven N Evans, and Montgomery Slatkin. Bayesian inference of natural selection from allele frequency time series. *Genetics*, 203(1):493–511, 2016.

Per Sjödin, Pontus Skoglund, and Mattias Jakobsson. Assessing the maximum contribution from ancient populations. *Molecular biology and evolution*, page msu059, 2014.

Pontus Skoglund, Helena Malmström, Maanasa Raghavan, Jan Storå, Per Hall, Eske Willerslev, M Thomas P Gilbert, Anders Götherström, and Mattias Jakobsson. Origins and genetic legacy of neolithic farmers and hunter-gatherers in europe. *Science*, 336(6080):466–469, 2012.

Pontus Skoglund, Helena Malmström, Ayça Omrak, Maanasa Raghavan, Cristina Valdiosera, Torsten Günther, Per Hall, Kristiina Tambets, Jüri Parik, Karl-Göran Sjögren, et al. Genomic diversity and admixture differs for stone-age scandinavian foragers and farmers. *Science*, 344(6185):747–750, 2014.

7 Appendix

7.1 Computing allele frequency moments in the ancient population

We wish to compute moments of the form

$$\mathbb{E}_x(g(Y); t_1, t_2) = \int_0^1 g(y) f(y; x, t_1, t_2) dy. \tag{4}$$

To do so, we make use of several results from diffusion theory. To ensure that this paper is self contained, we briefly review those results here. The interested reader may find much of this material covered in Ewens (2012); Karlin and Taylor (1981). Several similar calculations can be found in Griffiths (2003).

Let the probability of an allele going from frequency x to frequency y in τ generations in a population of size N_e be $f(x, y; t)$, where $t = \tau/(2N_e)$. Under a wide variety of models, the change in allele frequencies through time is well approximated by the Wright-Fisher diffusion, which is characterized by its generator,

$$\mathcal{L} = \frac{1}{2}x(1-x)\frac{d^2}{dx^2}.$$

The generator of a diffusion process is useful, because it can be used to define a differential equation for the moments of that process,

$$\frac{d}{dt}\mathbb{E}_x(g(X_t)) = \mathbb{E}_x\left(\mathcal{L}g(X_t)\right). \tag{5}$$

We will require the *speed measure* of the Wright-Fisher diffusion, $m(x) = x^{-1}(1-x)^{-1}$, which essentially describes how slow a diffusion at position x is "moving" compared to a Brownian motion at position x. Note that all diffusions are reversible with respect to their speed measures, i.e.

$$m(x)f(x, y; t) = m(y)f(y, x; t).$$

We additionally require the probability of loss, i.e. the probability that the allele currently at frequency x is ultimately lost from the population. This is

$$u_0(x) = 1 - x.$$

Note that it is possible to condition the Wright-Fisher diffusion to eventually be lost.

The transition density can be computed as

$$f^{\downarrow}(x, y; t) = f(x, y; t)\frac{u_0(y)}{u_0(x)}$$

by using Bayes theorem. The diffusion conditioned on loss is characterized by its generator,

$$\mathcal{L}^{\downarrow} = -x\frac{d}{dx} + \frac{1}{2}x(1-x)\frac{d^2}{dx^2}.$$

In an infinite sites model, in which mutations occur at the times of a Poisson process with rate $\theta/2$ and then each drift according to the Wright-Fisher diffusion, a quasi-equilibrium distribution will be reached, known as the frequency spectrum. The frequency spectrum, $\phi(x)$, predicts the number of sites at frequency x, and can be written in terms of the speed measure and the probability of loss,

$$\phi(x) = \theta m(x) u_0(x).$$

To proceed with calculating (4), note that the conditional probability of an allele being at frequency y in the ancient population given that it's at frequency x in the modern population can be calculated

$$f(y; x, t_1, t_2) = \frac{f(x, y; t_1, t_2)}{\phi(x)}$$

where $f(x, y; t_1, t_2)$ is the joint probability of the allele frequencies in the modern and ancient populations and $\phi(x)$ is the frequency spectrum in the modern population.

Assuming that the ancestral population of the modern and ancient samples was at equilibrium, the joint distribution of allele frequencies can be computed by sampling alleles from the frequency spectrum of the ancestor and evolving them forward in time via the Wright-Fisher diffusion. This can be written mathematically as

$$f(x, y; t_1, t_2) = \int_0^1 f(z, x; t_1) f(z, y; t_2) \phi(z) dz.$$

We now expand the frequency spectrum in terms of the speed measure and the probability of loss and use reversibility with respect to the speed measure to rewrite the equation,

$$\begin{aligned}\int_0^1 f(z,x;t_1)f(z,y;t_2)\phi(z)dz &= \theta\int_0^1 f(z,x;t_1)f(z,y;t_2)m(z)u_0(z)dz \\ &= \theta\int_0^1 \frac{m(x)}{m(z)}f(x,z;t_1)f(z,y;t_2)m(z)u_0(z)dz \\ &= \theta m(x)u_0(x)\int_0^1 f(x,z;t_1)\frac{u_0(z)}{u_0(x)}f(z,y;t_2)dz \\ &= \phi(x)\int_0^1 f^{\downarrow}(x,z;t_1)f(z,y;t_2)dz.\end{aligned}$$

The third line follows by multiplying by $u_0(x)/u_0(x) = 1$. This equation has the interpretation of sampling an allele from the frequency spectrum in the modern population, then evolving it *backward* in time to the common ancestor, before evolving it *forward* in time to the ancient population. The interpretation of the diffusion conditioned on loss as evolving backward in time arises by considering the fact that alleles arose from unique mutations at some point in the past; hence, looking backward, alleles must eventually be lost at some point in the past.

To compute the expectation, we substitute this form for the joint probability into (4),

$$\begin{aligned}\int_0^1 g(y)f(y;x,t_1,t_2)dy &= \int_0^1 g(y)\left(\int_0^1 f^{\downarrow}(x,z;t_1)f(z,y;t_2)dz\right)dy \\ &= \int_0^1 \left(\int_0^1 g(y)f(z,y;t_2)dy\right)f^{\downarrow}(x,z;t_1)dz,\end{aligned}$$

where the second line follows by rearranging terms and exchanging the order of integration. Note that this formula takes the form of nested expectations. Specifically,

$$\begin{aligned}\int_0^1 g(y)f(z,y;t_2)dy &= \mathbb{E}_z(g(Y_{t_2})) \\ &\equiv h(z)\end{aligned}$$

and

$$\int_0^1 h(z) f^{\downarrow}(x, z; t_1) dz = \mathbb{E}_x^{\downarrow}(h(Z_{t_1})) \\ = \mathbb{E}_x(g(Y); t_1, t_2).$$

We now use (5) to note that

$$\frac{d}{dt} p_{n,k} = \frac{k(k-1)}{2} p_{n,k-1} - k(n-k) p_{n,k} + \frac{(n-k)(n-k-1)}{2} p_{n,k+1}$$

and

$$\frac{d}{dt} p^{\downarrow}_{n,k} = \frac{k(k-1)}{2} p^{\downarrow}_{n,k-1} - k(n-k+1) p^{\downarrow}_{n,k} + \frac{(n-k+1)(n-k)}{2} p^{\downarrow}_{n,k+1}$$

with obvious boundary conditions $p_{n,k}(0; z) = z^k (1-z)^{n-k}$ and $p^{\downarrow}_{n,k}(0; x) = x^k (1-x)^{n-k}$.

These systems of differential equations can be rewritten as matrix differential equations with coefficient matrices Q and $Q^{\downarrow}$ respectively. Because they are linear, first order equations, they can be solved by matrix exponentiation. Because the expectation of a polynomial in the Wright-Fisher diffusion remains a polynomial, the nested expectations can be computed via matrix multiplication of the solutions to these differential equations, yielding the formula (2).

7.2 Robustness to ascertainment in the modern population

By conditioning on the allele frequency in the modern population, we gain the power to make inferences that are robust to ascertainment in the modern population. To see this, note from Equation 3 in Nielsen and Signorovitch (2003) that

$$f(x|A) = \frac{f(x, A)}{f(A)}$$

where A indicates the event that the allele was ascertained in the modern population. A simple generalization of this shows that

$$f(x, y|A) = \frac{f(x, y, A)}{f(A)}.$$

So,

$$\begin{aligned} f(y|x, A) &= \frac{f(x, y|A)}{f(x|A)} \\ &= \frac{f(x, y, A)}{f(x, A)} \\ &= \frac{f(A|x, y)f(x, y)}{f(A|x)f(x)} \\ &= \frac{f(x, y)}{f(x)} \end{aligned}$$

where the final line follows by recognizing that $f(A|x, y) = f(A|x)$ since the allele was ascertained in the modern population. Thus, we see that the ascertainment is removed by conditioning and we recover the original formula. Note that the robustness to ascertainment is only exact if the allele is ascertained in the modern population, but is expected to be very close to to true so long as the allele is ascertained in a population closer to the modern population than to the ancient population.

7.3 Sites covered exactly once have no information about drift in the ancient population

Consider a simplified model in which each site has exactly one read. When we have sequence from only a single individual, we have a set l_a of sites where the single read is an ancestral allele and a set l_d of sites where the single read is a derived allele. Thus, we can rewrite (3) as

$$L(D) = \prod_{l \in l_a} \left((1-\epsilon)P_{2,0}(x_l) + \frac{1}{2}P_{2,1}(x_l) + \epsilon P_{2,2}(x_l) \right) \prod_{l \in l_d} \left(\epsilon P_{2,0}(x_l) + \frac{1}{2}P_{2,1}(x_l) + (1-\epsilon)P_{2,2}(x_l) \right).$$

We can use formulas from Racimo et al. (2016) to compute $P_{2,k}(x_l)$ for $k \in \{0, 1, 2\}$,

$$
\begin{aligned}
P_{2,0}(x_l) &= 1 - x_l e^{-t_1} - \frac{1}{2} x_l e^{-(t_1+t_2)} + x_l \left(x_l - \frac{1}{2} \right) e^{-(3t_1+t_2)} \\
P_{2,1}(x_l) &= x_l e^{-(t_1+t_2)} + x_l (1 - 2x_l) e^{-(3t_1+t_2)} \\
P_{2,2}(x_l) &= x_l e^{-t_1} - \frac{1}{2} x_l e^{-(t_1+t_2)} + x_l \left(x_l - \frac{1}{2} \right) e^{-(3t_1-t_2)}.
\end{aligned}
$$

610 Note then that

$$
(1 - \epsilon) P_{2,0}(x_l) + \frac{1}{2} P_{2,1}(x_l) + \epsilon P_{2,2}(x_l) = 1 - \epsilon - x(1 - 2\epsilon) e^{-t_1}
$$

611 and

$$
\epsilon P_{2,0}(x_l) + \frac{1}{2} P_{2,1}(x_l) + (1 - \epsilon) P_{2,2}(x_l) = \epsilon + x(1 - 2\epsilon) e^{-t_1}.
$$

612 Neither of these formulas depend on t_2; hence, there is no information about the drift
613 time in the ancient population from data that is exactly 1x coverage.